Validation of a morphogenesis model of *Drosophila* early development by a multi-objective evolutionary optimization algorithm

Rui Dilão[1], Daniele Muraro[1], Miguel Nicolau[2], and Marc Schoenauer[2]

[1] Nonlinear Dynamics Group, IST
Department of Physics, Av. Rovisco Pais, Lisbon, Portugal
{rui,muraro}@sd.ist.utl.pt
[2] INRIA Saclay - Île-de-France
LRI- Université Paris-Sud, Paris, France
{Miguel.Nicolau,Marc.Schoenauer}@inria.fr

Abstract. We apply evolutionary computation to calibrate the parameters of a morphogenesis model of *Drosophila* early development. The model aims to describe the establishment of the steady gradients of Bicoid and Caudal proteins along the antero-posterior axis of the embryo of *Drosophila*. The model equations consist of a system of non-linear parabolic partial differential equations with initial and zero flux boundary conditions. We compare the results of single- and multi-objective variants of the CMA-ES algorithm for the model the calibration with the experimental data. Whereas the multi-objective algorithm computes a full approximation of the Pareto front, repeated runs of the single-objective algorithm give solutions that dominate (in the Pareto sense) the results of the multi-objective approach. We retain as best solutions those found by the latter technique. From the biological point of view, all such solutions are all equally acceptable, and for our test cases, the relative error between the experimental data and validated model solutions on the Pareto front are in the range $3\% - 6\%$. This technique is general and can be used as a generic tool for parameter calibration problems.

1 Introduction

The ultimate validation of mathematical or computational models of real Complex Systems can only be achieved by comparing the outcomes of the models with those of the actual system. Such models generally depend on several parameters that must be identified using experimental data. System calibration is the search for the set of parameters such that the output of the model best fits the available data. Ideally, in order to avoid possible over-fitting of the model to the data, system calibration should be performed using a data set, and the validation of the model should be done using other data sets not used during the calibration.

This paper deals with the validation and calibration of a reaction-diffusion model for the spatial distribution of proteins during the early stage of morphogenesis of *Drosophila*. This model incorporates the regulatory repression mechanism of Bicoid protein over *caudal* mRNA. In this case, several experimental data sets for both Bicoid and Caudal proteins are available.

Model calibration from experimental data can be formulated as an optimization problem — find the model that minimizes the difference between its outputs and the experimental data [MSM97]. Such optimization problems are usually highly multi-modal, and classical methods (e.g. gradient-based techniques) fail to give reliable solutions. Therefore, Evolutionary Algorithms (EAs) are a better choice.

In the case analyzed here, we have experimental data for the distribution of both Bicoid and Caudal proteins along the antero-posterior axis of the embryo of

Drosophila. An ideal set of parameters for the perfect model would reach the best possible fit for both distribution, and the calibration problem could be turned into a standard optimization problem involving both fits by minimization of the sum of the Mean Square Errors (MSEs) of both models calculated with the data for both distributions. However, we are looking for meaningful biological parameters rather than for the best set of parameters. Moreover, it is likely that the orders of magnitude or the experimental errors on both proteins differ, and a simple linear aggregation of MSEs might give unbalanced results between both proteins. Therefore, a multi-objective approach seems more appropriate for our gols of model calibration and validation. On the other hand, it has been shown that the multi-objectivization of a fitness function can reduce the number of local optima [HLK08].

In order to validate these arguments, we compare the results of a single-objective approach (minimizing some weighted sums of both MSEs) to those of a multi-objective algorithm. Each trial of single-objective minimization allows us to identify one point close to the Pareto front, and hence several trials, together with good guesses for the weights of the aggregation, are necessary to sample the Pareto front reliably. The multi-objective approach lead to a full set of solutions that are hopefully close to the Pareto front. However, it turns out that for this calibration problem, a simple single-objective strategy seems to outperform better than the multi-objective approach.

This paper is structured as follows. Section 2 gives a brief description of the meaningful biological mechanisms involved in the *Drosophila* early development. Section 3 derives the reaction-diffusion model describing the production of Bicoid and Caudal from mRNAs. The parameters in the reaction-diffusion equations are to be calibrated with the experimental data. Initial conditions are given as piecewise constant functions and will be also fitted with the evolutionary algorithm. Section 4 introduces the evolutionary single- and multi-objective optimization algorithms. Section 5 applies both algorithms to the calibration of the model and compares the results. Finally, in section 6, we discuss the main conclusions of the paper.

2   Biological Background

Morphogenesis in *Drosophila* early development begins with the deposition of *bicoid* mRNA of maternal origin near one of the poles of the embryo [NV96]. During the first two hours of development, a sequence of 14 mitotic nuclear replication cycles occurs without the formation of cellular membranes around the nuclei. The early formed nuclei of the embryo lie in a single cell — the syncytial blastoderm. The nuclear membranes only appear at the end of the 14th mitotic cycle.

The absence of cellular membranes facilitates the diffusion of substances in the embryo and, during the syncytial stage, stable gradients of proteins are established. In later stages of development, the formation of the head, of the thorax and of the abdomen are associated with the patterns of distribution of proteins that took place during the previous syncytial stage of development.

After fertilization of the egg, the localized *bicoid* mRNA is translated into Bicoid protein and this protein regulates the transcription of the other zygotic genes. Other proteins of maternal origin as Caudal, Nanos or Hunchback, are produced in the early syncytial stage and are regulated by Bicoid.

During mitotic cycles 11 to 14, the observed distribution of proteins along the antero-posterior axis of *Drosophila* shows a high concentration near the nuclear membranes and a low concentration in the space between nuclei, Figure 1a and 1b.

In order to explain the observed protein gradients, a mRNA diffusion model has been proposed [DM09]. In this model, mRNA diffuses along the embryo and the produced protein stay localized near the nuclei of the mebryo. As the developmental process proceeds in time, proteins reach a steady gradient-like distribution.
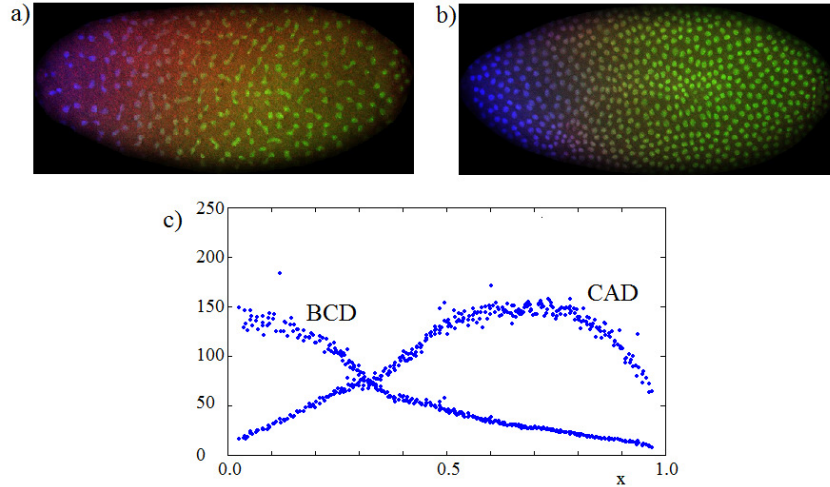
Fig. 1. Localization of Bicoid (blue) and Caudal (green) proteins near the nuclear membrane of the embryo of *Drosophila* after mitotic cycles number 11 (a) and 12 (b). This picture was taken from the datasets ab18 (a) and ab17 (b) of the FlyEx database (http://flyex.ams.sunysb.edu/flyex/, [MKRS99] and [MSKSR01]). From 1a to 1b, the nuclei have divided by mitosis, but the proteins remain sticked to the region around the nuclear membranes. In c), we show the steady state concentrations of proteins Bicoid (BCD) and Caudal (CAD) along the antero-posterior axis (x) of the embryo of *Drosophila*. This distribution has been extracted from the data set ad13 (FlyEx database), corresponding to a late stage of the mitotic cycle number 14. The horizontal axis has been scaled to the embryo length $L = 1$, and the vertical scale corresponds to light intensity arbitrary units.

Developmental processes are in general associated with the production of a cascade of regulatory processes involving genes, mRNAs and proteins. In nowadays experiments, these regulatory dependencies are specifically addressed. The simplest example is the repression effect of protein Bicoid over *caudal* mRNA, [RPJ96], Figure 1c). In this paper, we model the relationship between Bicoid and Caudal through the repression mechanism, and we further calibrate it with experimental data.

3   The Mathematical Model

During the first stage of development of *Drosophila*, the processes occurring in the embryo can be modelled in an one-dimensional domain of length L, representing the antero-posterior axis of the embryo. The *bicoid* (*bcd*) and *caudal* (*cad*) mRNA of maternal origin have initial distributions given by,

$$bcd(x, t = 0) = \begin{cases} A > 0, \text{ if } 0 < L_1 < x < L_2 < L \\ 0, \qquad \text{otherwise} \end{cases}$$
$$cad(x, t = 0) = \begin{cases} C > 0, \text{ if } 0 < L_3 < x < L_4 < L \\ 0, \qquad \text{otherwise} \end{cases} \tag{1}$$

where L_1, L_2, L_3 and L_4 are constants defining the intervals of localization of the corresponding mRNA, and A and C are concentration constants. These distributions of mRNAs correspond to a precise initial localization as shown in experiments.

During the first stage of development, *bicoid* and *caudal* mRNAs are transformed into proteins with rate constants a_{bcd} and a_{cad}. This transformation occurs in the ribosomes, in general localized near nuclear membranes. The presence of the protein

Bicoid prevents the expression of Caudal through a repression mechanism ([RPJ96]) that can be described by the mass action type transformation,

$$BCD + cad \xrightarrow{r} BCD \qquad (2)$$

where r is a rate of degradation.

Introducing the hypothesis that mRNA diffuses and proteins stay localized in the embryo, and with the additional repression mechanism (2), the concentration of proteins and mRNAs in these processes evolves in time according to the model equations,

$$\begin{cases} \dfrac{\partial bcd}{\partial t} &= -a_{bcd}bcd(x) + D_{bcd}\dfrac{\partial^2 bcd}{\partial x^2} \\ \dfrac{\partial BCD}{\partial t} &= a_{bcd}bcd(x) \\ \dfrac{\partial cad}{\partial t} &= -a_{cad}cad(x) - rBCD.cad + D_{cad}\dfrac{\partial^2 cad}{\partial x^2} \\ \dfrac{\partial CAD}{\partial t} &= a_{cad}cad(x) \end{cases} \qquad (3)$$

where D_{bcd} and D_{cad} are the diffusion coefficients of *bicoid* and *caudal* mRNAs, respectively. Capital letter symbols refer to protein concentrations, and lower case italic letters to mRNA concentrations.

In order to calibrate the model equations just derived in (3) with the experimental profiles, as the ones in Figure 1c), we have to identify the parameters of protein production (a_{bcd} and a_{cad}), the parameter of repression (r), the initial distribution of mRNAs (1), the ratio between the diffusion coefficients (D_{bcd}/D_{cad}, see [DJ98]), and the time, considered here as a parameter.

An ideal set of parameters calibrating an exact model with ideal experimental data would reach the best possible fit for both distributions (a zero-error fit), the calibration problem could simply be turned into a standard optimization problem involving both fits through the minimization of the sum of Mean Square Errors for both distributions. However, as in general the model is not exact, the data are noisy, and the experimental errors of both proteins might differ even by some orders of magnitude, the simple weighted sums of MSEs might give unbalanced results between both proteins.

The goal here is to find a set of parameters whose fit for both proteins has an error under a reasonable error margin, and to select an ensemble of parameters that are equivalent and well distributed inside this set of parameters. Such a goal can be rigorously defined in the setting of *multi-objective* or *Pareto optimization*.

In the following, we fit the parameters of model equations (3) for the distribution of proteins Bicoid and Caudal, with single- and multi-objective approaches. We compare the errors and computational efforts of both approaches.

4   The algorithms

In this section, we introduce the algorithms that have been used to calibrate the model derived in the previous section. Both are based on the *Covariance Matrix Adaptation Evolution Strategy* (CMA-ES) algorithm [HO01], an Evolutionary Algorithm for black-box continuous optimization. The first algorithm is for single-objective optimization, and will be referred as CMA-ES. The second algorithm is a multi-objective version of CMA-ES, and uses embedded CMA-ES processes, together with a global Pareto-dominance based selection [IHR07].

4.1 Single-objective optimization: CMA-ES

Since we are dealing here with continuous optimization, the best choice of an evolutionary method is the Covariance Matrix Adaptation Evolution Strategy (CMA-ES), first introduced in the mid-90s by Hansen and Ostermeier [HOG95,HO96], and that has reached maturity in the early 00's [HO01,HMK03,AH05]. Results from the CEC 2005 competition [Han05] and further systematic comparisons [HRM08], have shown that, thanks to its ES invariance properties, CMA-ES outperforms better than most other methods on artificial benchmarks with tunable difficulties, as well as on many real-world problems from different scientific domains.

CMA-ES is a $(\mu, \lambda)-$Evolution Strategy [Sch81], in the sense that it is an EA that uses a population of μ parents to generate λ offspring, and deterministically selects the best μ of those λ offspring for the next generation. As in all Evolution Strategies (ES), the offspring are generated by sampling a Gaussian distribution. However, in CMA-ES, this distribution is centered on a weighted recombination of the μ parents. Moreover, multidimensional Gaussian distributions are determined by their covariance matrix, a positive definite symmetrical matrix, and the art of ES lies in the way the parameters of this Gaussian mutation (i.e. the covariance matrix) are adapted on-line: CMA-ES uses the notion of *cumulated path*, i.e. modifies the matrix such that previous good moves become more likely (for further details see [HO01]). One of the important properties of CMA-ES is that it is independent of the coordinate system (*rotation-invariant*).

4.2 Evolutionary Pareto Optimization

Pareto optimality is a concept introduced by Vilfredo Pareto to evaluate the efficiency of an economic system, with applications in game theory, engineering and social sciences. It is at stake in the process of simultaneously optimizing several conflicting objectives subject to certain constraints. Pareto optimization is concerned in finding the set of *optimal trade-offs* between conflicting objectives, i.e., solutions such that the value of one objective cannot be improved without degrading the value of at least another objective. Such best compromises are what is called the *Pareto set* of the multi-objective optimization problem.

Pareto optimization is based on the notion of *dominance*. Consider a minimization problem with M real valued objective functions $f = (f_1, \ldots, f_M)$, defined on a subset $X \subset \mathbb{R}^N$, $f : X \subset \mathbb{R}^N \to \mathbb{R}^M$. A solution $x \in X$ is said to *dominate* $\bar{x} \in X$, (denoted by $x \prec \bar{x}$), if,

$$(\forall m \in \{1, \ldots, M\} : f_m(x) \leq f_m(\bar{x})) \wedge (\exists m \in \{1, \ldots, M\} : f_m(x) < f_m(\bar{x})) \ .$$

The goal of Pareto optimization is to find a good approximation to the *Pareto set*, the set of non-dominated points of the search space, generating a set of solutions in such a way that the objective values are as uniformly distributed as possible on the *Pareto front*, the image of the Pareto set in the objective space.

The classical approach of reducing the multi-objective problem into a mono-objective one by linearly aggregating all the objectives in a scalar function might provide only a subset of the Pareto optimal solutions, as for instance it does not allow to sample the concave regions of the Pareto front [DD97]. A better idea is to use the Pareto dominance relation to select the most promising individuals within an evolutionary algorithm. Unfortunately, the dominance relation is only a partial order relation, i.e., in many cases, neither A dominates B, nor B dominates A. A secondary selection criterion is hence needed in order to get a total order relation over the search space. Many different approaches have been proposed in the last

decade (see e.g. [Deb01] and [CVL02] for recent textbooks), and Evolutionary Multi-Objective Optimization is considered today a stand-alone branch of Evolutionary Algorithms with specialized workshops and conference series.

Because Covariance Matrix Adaptation was proven so successful for (single-objective) evolutionary continuous optimization, and because a multi-objective version of the algorithm has been recently proposed [IHR07], it seemed a good choice for the calibration problem at hand here.

4.3   Multi-Objective CMA-ES

The Multi-Objective CMA-ES (MO-CMA-ES) [IHR07] is based on a specific (1+1)-CMA-ES algorithm, a simplified version of CMA-ES where the number of parents is set to 1, and the update of the stepsize uses a simple rule based on Rechenberg's well-known 1/5th rule [Rec73]. λ_{MO} (1+1)-CMA-ES are run in parallel, each with its own stepsize and covariance matrix. At each generation, each parent generates one offspring, and updates its mutation parameters. Then the set of λ_{MO} parents and their λ_{MO} offspring are ranked together according to the chosen selection criterion, and the best λ_{MO} carry on to the next generation.

The selection criterion goes as follows. The first sorting criterion, based on the Pareto dominance, is the non-dominated sorting proposed with NSGA-II algorithm [DPA02]: all non-dominated individuals are given rank one, and removed from the population. Amongst remaining individuals, the non-dominated ones are given rank 2, and the procedure continues until the number of required individuals is reached (λ_{MO} here). With a fast non dominated sorting approach the computational time needed to rank a population of size N can be kept of the order of MN^2 where M is the number of the objectives (see [DPA02]).

However, a second criterion is necessary, firstly in order to rank the solutions within the same rank of non-dominance, but also (and more importantly here) to guarantee a distribution as uniform as possible in the region of the objective space occupied by the Pareto front. In [IHR07] two criteria are examined: the *crowding distance* and the *contributing hypervolume*.
The crowding distance has been proposed by [DPA02] for the NSGA-II algorithm, and ranks the solutions depending on their distances to their immediate neighbors in the objective space.

Another approach is to use a metric called *S-metric* or *hypervolume measure* introduced by Zitler and Thiele [ZT98] which gives the "size of the objective value space which is covered by a set of non-dominated solutions". More precisely, it is the Lebesgue measure Λ of the union of the hypercubes a_i defined by the non-dominated points m_i and a reference point x_{ref} (see Figure 2):

$$S(\mathcal{D}) := \Lambda\big(\{\bigcup_{i=1}^{\#\mathcal{D}} a_i : m_i \in \mathcal{D}\}\big) = \Lambda\big(\bigcup_{m \in \mathcal{D}} \{x : m \prec x \prec x_{ref}\}\big)$$

where $\mathcal{D}$ is the set of the non-dominated points.

In [Fle03], Fleischer proved that the maximization of S constitutes a necessary and sufficient condition for the objectives to be maximally diverse Pareto optimal solutions of discrete, multi-objective, optimization problem, and proposed an algorithm to evaluate the hypervolume measure of a set in a polynomial time $O(K^3 M^2)$, where K is the number of solutions in the Pareto set and M is the number of objectives. This algorithm can be efficiently implemented by an archiving strategy [KCF03]. In such a way the multi-objective problem is reduced to the single-objective one of maximizing the hypervolume measure. This measure also provides a unary indicator on the degree of success of the algorithm enabling the comparison with the results of other multi-objective algorithms.
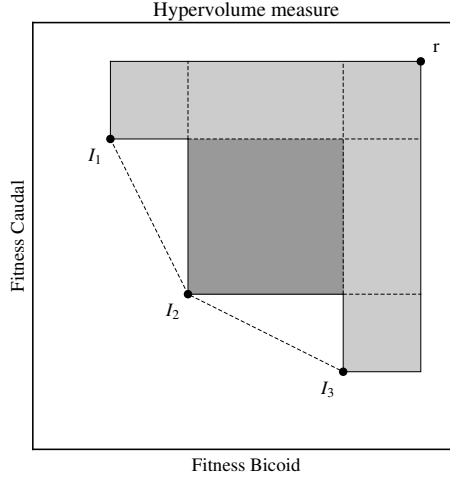
Fig. 2. The hypervolume measure is "the size of the objective value space which is covered by a set of non-dominated solutions" from a reference point (r). In light and dark grey the hypervolume measure of three non-dominated individuals I_1, I_2, I_3. In dark grey the contributing hypervolume of the individual I_2.

According to [IHR07], after several tests on both criteria with two unary indicators, namely the hypervolume and the ϵ-indicator, "selection based on the hypervolume seems to be superior".

5 Experimental Calibration of the Model

5.1 The objectives

We have applied and compared two multi-objective strategies for the calibration of the parameters in model equations (3). The experimental data has been taken from the FlyEx database, [MKRS99] and [MSKSR01]. We have tested two algorithms on the distributions of the proteins Bicoid and Caudal along the antero-posterior axis of the embryo of *Drosophila* during cleavage cycle 14 (embryo ad13, see Figure 1). We describe these distributions by the numerical solutions of equations (3), determined by the techniques developed in [DJ98]. In order to keep the calibration as little biased as possible, we have set the number of integration steps as an unknown parameter. In this case, we are not assuming that Bicoid and Caudal protein distributions are in a steady state.

We denote by $BCD(x, \boldsymbol{\alpha})$ and $CAD(x, \boldsymbol{\alpha})$ the results of the numerical integration of equations (3), where $x \in [0, 1]$ and $\boldsymbol{\alpha} = (\alpha_1, \dots, \alpha_m)$ is the set of parameters to be determined. The parameter search space is a hyper-rectangle in $\mathbb{R}^m$, and we denote by $\{(x_i, BCD_{exp}(x_i))\}_{i=1}^n$ and $\{(x_i, CAD_{exp}(x_i))\}_{i=1}^n$ the experimental data points. The calibration of the parameters for the model equation (3) is thus reduced to a bi-objective optimization problem, minimizing the fitness functions,

$$FitBCD(\boldsymbol{\alpha}) = \frac{1}{n} \sum_{i=1}^{n} (BCD(x_i, \boldsymbol{\alpha}) - BCD_{exp}(x_i))^2$$

$$FitCAD(\boldsymbol{\alpha}) = \frac{1}{n} \sum_{i=1}^{n} (CAD(x_i, \boldsymbol{\alpha}) - CAD_{exp}(x_i))^2$$

5.2 The strategies

The **multi-objective strategy** uses MO-CMA-ES (Section 4.3) with a population size of $\lambda_{MO} = 100$. However, as we are not interested in the extreme parts of the Pareto Front, that have very low error value for one protein at the cost of a very high error on the other, we added a penalization to gradually eliminate large error values. More precisely, the target was to sample the Pareto front in the range $[0, 40] \times [0, 80]$ (bounds chosen after some preliminary runs), and we penalized $FitBCD$ (resp. $FitCAD$) by the amount by which $FitCAD$ (resp. $FitBCD$) overpassed its upper bound.

In total, the algorithm has been run 100 times, then the non-dominated points were extracted from the 100 populations, grouped together, leading to what can be seen as the best approximation of the Pareto Front by MO-CMA-ES.

As for the **single-objective strategy**, we used a standard aggregation technique: We have repeatedly executed CMA-ES for a family of single-objective fitness functions defined by a set of lines in the objective space with slopes c_i, namely,

$$Fit(\boldsymbol{\alpha}, c_i) = FitCAD(\boldsymbol{\alpha}) + c_i \cdot FitBCD(\boldsymbol{\alpha}), \qquad \text{where } i = 1, \ldots, 5$$

12 different slopes have been used $(0.01, 1, 5, 10, 25, 50, 60, 70, 75, 80, 90, 100)$, with 10 runs for each slope. In the end, the best results obtained for each slope has been gathered together, and the non-dominated ones are considered to be the best possible approximation of the Pareto Front for this strategy.
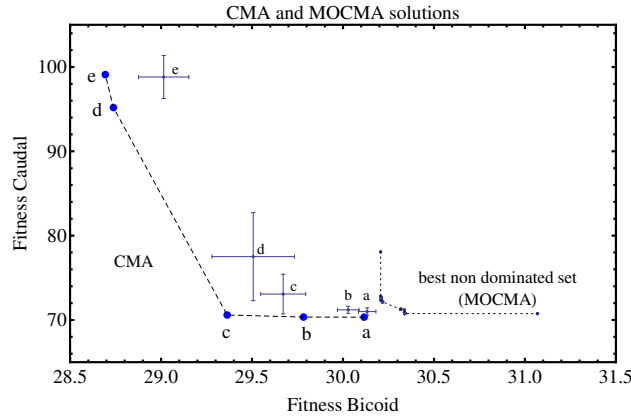
Fig. 3. Best non-dominated sets found by the single-objective (CMA) and multi-objective (MO-CMA) techniques. In the single-objective approach, we have optimized the fitness function $FitCAD + c_i \cdot FitBCD$, for $c_i = 1, 5, 25, 50, 100$. By construction, the Pareto front is tangent to these lines. The results are labelled as small a, b, c, d, e, respectively. For each slope c_i, the mean values and the standard deviations are represented with crosses. The best result of each set of 10 optimization runs for each c_i has the same label. The final result of the multi-objective case is the best non-dominated population calculated by the intersection of the final populations of 100 independent runs. In this case, the MO-CMA technique gives worst solutions for the optimization problem.

5.3 Results

Figure 3 presents the results of both strategies, in objective space: the approximation of the Pareto Front by MO-CMA-ES is concentrated around 8 points only, and 5 points (a-e) represent the best approximation of the Pareto Front by CMA-ES,

corresponding to the slopes $(1, 5, 25, 50, 100)$. For each of these, the crosses represent the average values over the 10 runs along with standard deviations in both directions.

The first conclusion to be drawn is that MO-CMA-ES results are dominated by the CMA-ES results. Moreover, and this is the reason why so few slopes below 1 were tried, the results with slope 0.01 are slightly dominated, but very close to those with slope 1 (hence they are not plotted on Figure 3). This seems to indicate that $FitCAD$ has orders of magnitude more influence on the fits than $FitBCD$. In order to confirm this point, we ran CMA-ES on each fitness alone: it reaches error values down to $FitCAD = 47$, but at the cost of an error on Bicoid of order 10^6 - while $FitBCD$ never reached any value lower than 28.
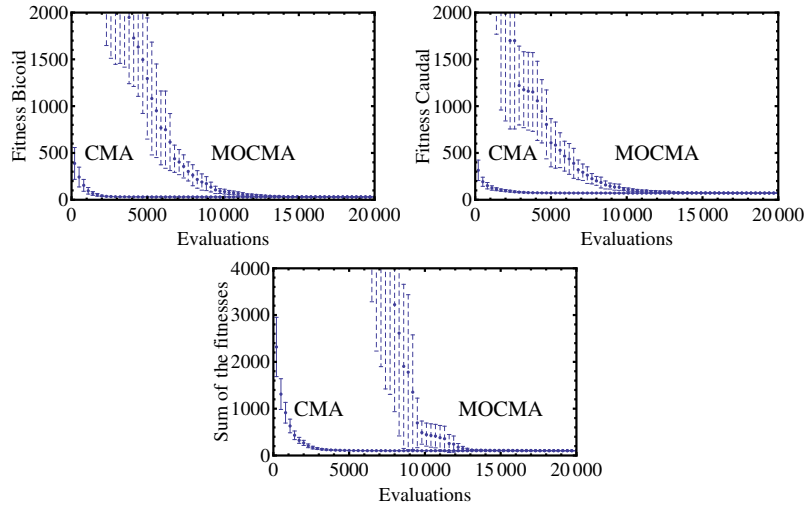
Fig. 4. Evolution of the fitnesses (MSEs on the Bicoid and Caudal) during optimization. Plotted are the averages and standard deviations over 100 runs for both CMA-ES, minimizing the sum of both fitnesses, and MO-CMA-ES. Above are single fitness values (the minimal values in the population for MO-CMA-ES, the values for the best individual in CMA-ES). Below is the sum of both of the above (the actual fitness used by CMA-ES).

Another finding was that the final populations of the MO-CMA-ES runs (not shown) were very diverse, whereas all single-objective runs for the same slope robustly found very similar solutions, as witnessed by the crosses on Figure 3. MO-CMA-ES seems to lack some evolutionary pressure toward the true Pareto Front, maybe because, in multi-objective algorithms, the whole population rapidly contains only non-dominated points, and the selection pressure is then enforcing the uniform spreading on the current front rather than progress toward the true Pareto Front.

Figure 4 illustrates the situation, by plotting average results for 100 runs of MO-CMA-ES on the one hand, and of CMA-ES optimizing $FitCAD(\boldsymbol{\alpha}) + FitBCD(\boldsymbol{\alpha})$ (i.e. corresponding to point a in figure 3) on the other hand. Above plots are the best values in the population (averaged over the 100 runs) for $FitCAD$ and $FitBCD$, and below is the sum of both. The fact that the MO-CMA-ES plot never catches up that of CMA-ES, even when considering the best possible value for one error alone, is another sign of its poor behavior.

Note that both algorithms are compared using the number of function evaluations on the x-axis, but the MO-CMA-ES requires some additional overhead time:

the update of the covariance matrix is made for each individual, and the whole population undergoes non-dominated sorting. However, for larger systems of differential equations, such as the ones describing the genetic network of the early development of *Drosophila*, [AD06], the computational cost of numerical integration will be the most time consuming part of the algorithm. This is why it has also been used here.

Table 1 displays the parameters of model equations (3) and the corresponding fitness values, fitted with the CMA-ES algorithm. The actual fits of the corresponding solutions of the model equations (3) and plotted against experimental data are shown in Figure 5. In the numerical fits, we have fixed the *Drosophila* embryo length to the standard value $L = 0.5 \times 10^{-3} m$, and all the graphs of Figure 5 have been scaled to the interval $[0, 1]$.

|	a	b	c	d	e	mean	σ
L_1	$5.68 \cdot 10^{-2}$	$6.72 \cdot 10^{-2}$	$6.25 \cdot 10^{-2}$	$3.29 \cdot 10^{-2}$	$1.43 \cdot 10^{-2}$	$4.67 \cdot 10^{-2}$	$2.24 \cdot 10^{-2}$
L_2	$1.73 \cdot 10^{-1}$	$1.68 \cdot 10^{-1}$	$1.62 \cdot 10^{-1}$	$1.84 \cdot 10^{-1}$	$1.94 \cdot 10^{-1}$	$1.76 \cdot 10^{-1}$	$0.12 \cdot 10^{-1}$
L_3	$4.28 \cdot 10^{-1}$	$4.35 \cdot 10^{-1}$	$4.04 \cdot 10^{-1}$	$4.07 \cdot 10^{-1}$	$4.04 \cdot 10^{-1}$	$4.16 \cdot 10^{-1}$	$0.14 \cdot 10^{-1}$
L_4	$7.63 \cdot 10^{-1}$	$7.74 \cdot 10^{-1}$	$8.45 \cdot 10^{-1}$	$8.45 \cdot 10^{-1}$	$8.48 \cdot 10^{-1}$	$8.15 \cdot 10^{-1}$	$0.42 \cdot 10^{-1}$
B	$1.53 \cdot 10^{+3}$	$1.98 \cdot 10^{+3}$	$3.47 \cdot 10^{+3}$	$2.36 \cdot 10^{+3}$	$1.98 \cdot 10^{+3}$	$2.26 \cdot 10^{+3}$	$0.73 \cdot 10^{+3}$
C	$1.06 \cdot 10^{+3}$	$1.08 \cdot 10^{+3}$	$1.26 \cdot 10^{+3}$	$1.28 \cdot 10^{+3}$	$1.28 \cdot 10^{+3}$	$1.19 \cdot 10^{+3}$	$0.11 \cdot 10^{+3}$
D_{bcd}	$1.00 \cdot 10^{-2}$	$1.09 \cdot 10^{-2}$	$1.99 \cdot 10^{-2}$	$2.03 \cdot 10^{-2}$	$2.04 \cdot 10^{-2}$	$1.63 \cdot 10^{-2}$	$0.53 \cdot 10^{-2}$
D_{cad}	$1.00 \cdot 10^{-2}$	$1.00 \cdot 10^{-2}$	$1.00 \cdot 10^{-2}$	$1.00 \cdot 10^{-2}$	$1.00 \cdot 10^{-2}$	$1.00 \cdot 10^{-2}$	$0.00 \cdot 10^{-2}$
a_{bcd}	$9.99 \cdot 10^{+4}$	$9.99 \cdot 10^{+4}$	$9.99 \cdot 10^{+4}$	$9.99 \cdot 10^{+4}$	$9.99 \cdot 10^{+4}$	$9.99 \cdot 10^{+4}$	$1.31 \cdot 10^{+1}$
a_{cad}	$9.99 \cdot 10^{+4}$	$9.99 \cdot 10^{+4}$	$9.99 \cdot 10^{+4}$	$9.99 \cdot 10^{+4}$	$9.99 \cdot 10^{+4}$	$9.99 \cdot 10^{+4}$	$3.96 \cdot 10^{+1}$
r	$8.64 \cdot 10^{+3}$	$6.74 \cdot 10^{+3}$	$3.34 \cdot 10^{-2}$	$5.74 \cdot 10^{-2}$	$6.71 \cdot 10^{-4}$	$3.07 \cdot 10^{+3}$	$4.26 \cdot 10^{+3}$
Iterations	$9.84 \cdot 10^{+3}$	$9.79 \cdot 10^{+3}$	$9.37 \cdot 10^{+3}$	$9.35 \cdot 10^{+3}$	$9.36 \cdot 10^{+3}$	$9.54 \cdot 10^{+3}$	$0.25 \cdot 10^{+3}$

Table 1. Parameter values for the five best non-dominated solutions of model equations (3), obtained with the CMA algorithm, for the experimental data set of Figure 1c). In Figure 5, we show this data set together with the solutions of equations (3) for the parameter values a-e. All the different choices of these parameter values are calibrated candidates of the experimental data set. We also show, for each parameter, the mean value (mean) and the standard deviation (σ) taken on the Pareto front.

The mean relative error between the experimental data and the optimized solutions of the model equations (3) can be measured by the fitness function. For example, for the case of Bicoid protein, if BCD_{max} is the maximum value of the experimental values, the relative error of the calibrated model equations can be measured by $\sqrt{FitBCD/BCD_{max}^2}$. For the experimental data analyzed here, the mean relative error of all solution in the approximated Pareto front using the single-objective strategy are in the range $3\% - 6\%$.

6   Discussion and conclusion

We have tested the applicability of a single- and a multi-objective algorithms to the calibration of a model equation for a biological process. We have used two approaches: reducing the multi-objective optimization problem to a parametrized single-objective problem, repeatedly tackled by CMA-ES algorithm; and use an *ab-initio* multi-objective perspective, the multi-objective version of CMA-ES.

From a Computer Science perspective, the most striking fact is the difference in performance between both algorithms. Further experiments with other multi-objective algorithms should be run before any conclusion can be drawn. However,
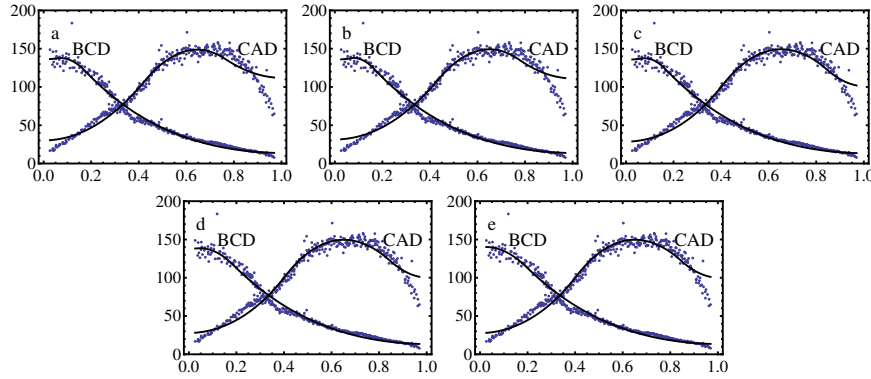
Fig. 5. Fits with experimental data for Bicoid and Caudal from the data shown in Figure 1c). (Embryo ad13 from the FlyEx database). The five figures correspond to the parameter values a-e in Table 1. The parameters of the different functions are on the best approximated Pareto set of Figure 3. In (a), we show the best fit for Bicoid and the worst fit for Caudal, then a gradual variation occurs, and in (e) it we have plotted the worst fit for Bicoid and the best fit for Caudal.

in this paper, the multi-objective approach lacks pressure toward the Pareto front, suggesting that other algorithms with a better control of the convergence to the Pareto front should be tried. Another important issue that must be tested is the generalization issue, i.e. how well the parameters that have been identified using one experimental dataset fit another dataset gathered from the same biological system.

From the biological point of view, we have shown that, if multi-objectives are considered, biological data is compatible with a large set of parameters values associated with a specific model. This non-dominated variability, intrinsic to biological systems, can explain the phenotypic plasticity of living systems.

On the other hand, from a more practical point of view, this problem enabled us to show the applicability of an mRNA diffusion model in order to describe the establishment of steady gradients of proteins in *Drosophila* early development.

Acknowledgements

References

[AD06] F. Alves and R. Dilão: Modelling segmental patterning in Drosophila: Maternal and gap genes. *Journal of Theoretical Biology*, 241 (2006) pp. 342–359

[CVL02] C. A. Coello Coello, D. A. Van Veldhuizen, and G.B. Lamont: Evolutionary algorithms for solving multi-objective problems. Kluwer Academic Publishers.

[DD97] I. Das, J. E. Dennis: A closer look at drawbacks of minimizing weighted sums of objectives for pareto set generation in multicriteria optimization problems. Structural optimization, Vol. **14**, No. 1. (1997) pp. 63–69

[Deb01] K. Deb: Multi-objective optimization using evolutionary algorithms. Wiley. (2001)

[DPA02] K. Deb, A. Pratap, S. Agarwal, and T. Meyarivan: A Fast and Elitist Multiobjective Genetic Algorithm: NSGA-II. IEEE Transactions on Evolutionary Computation, Vol. **6**, No. 2. (2002)

[DM09] R. Dilão and D. Muraro: Calibration and validation of mathematical models describing the gradient of Bicoid in the embryo of *Drosophila*. Pre-print, 2009.

[DJ98] R. Dilão and J. Sainhas: Validation and Calibration of Models for Reaction-Diffusion Systems. Int. J. of Bifurcation and Chaos, Vol. **8**. (1998) pp. 1163-1182

[EBN05] M. Emmerich, N. Beume, and B. Naujoks: An EMO Algorithm Using the Hypervolume Measure as Selection Criterion. In: C. A. Coello Coello et al. (Eds.): EMO 2005, LNCS 3410. Springer-Verlag. (2005) pp. 62–76

[Fle03] M. Fleischer: The Measure of Pareto Optima. Applications to Multi-objective Metaheuristics. In C. M. Fonseca et al. (Eds.): Evolutionary Multi-Criterion Optimization. Second International Conference, EMO 2003, Faro, Portugal. Lecture Notes in Computer Science, Vol. 2632. Springer. (2003) pp. 519–533

[HLK08] J. Handl, S.C. Lovell, and J. Knowles: Investigations into the Effect of Multi-objectivisation in Protein Structure Prediction. In G. Rudolph et al. (Eds), Parallel Problems Solving from Nature X, Dortmund, Germany. Lecture Notes in Computer Science, Vol. 5199. Springer Verlag. (2008) pp. 702–711

[HOG95] N. Hansen, A. Ostermeier, and A. Gawelczyk: On the Adaptation of Arbitrary Normal Mutation Distributions in Evolution Strategies: The Generating Set Adaptation. In: *ICGA95*. (1995) pp. 57–64

[HO96] N. Hansen, and A. Ostermeier: Adapting arbitrary normal mutation distributions in evolution strategies: The covariance matrix adaptation. In: *ICEC96*. IEEE Press. (1996) pp. 312–317

[HO01] N. Hansen, and A. Ostermeier: Completely Derandomized Self-Adaptation in Evolution Strategies. Evolutionary Computation, Vol. **9**, No. 2. (2001) pp. 159–195

[HMK03] N. Hansen, S. Müller and P. Koumoutsakos: Reducing the Time Complexity of the Derandomized Evolution Strategy with Covariance Matrix Adaptation (CMA-ES). Evolutionary Computation, Vol. **11**, No. 1. (2003)

[AH05] A. Auger, and N. Hansen: A Restart CMA Evolution Strategy With Increasing Population Size. In: *CEC'05*. IEEE Press. (2005) pp. 1769–1776

[Han05] N. Hansen et al.: Comparison of Evolutionary Algorithms on a Benchmark Function Set. In: *CEC'05 Special Session*. (2005)

[HRM08] N. Hansen, R. Ros, N. Mauny, M. Schoenauer, and A. Auger: PSO Facing Non-Separable and Ill-Conditioned Problems. INRIA Research Report number RR-6447. (2008)

[IHR07] C. Igel, N. Hansen, and S. Roth: Covariance Matrix Adaptation for Multi-objective Optimization. Evolutionary Computation, Vol. **15**, No. 1. (2007) pp. 1–28

[KCF03] J. D. Knowles, D. W. Corne, and M. Fleisher: Bounded Archiving using the Lebesgue Measure. Proceedings of CEC'2003, Vol. 4. IEEE Press. (2003) pp. 2490–2497

[MKRS99] E. Myasnikova, D. Kosman, J. Reinitz, M. Samsonova, 1999. Spatio-temporal registration of the expression patterns of *Drosophila* segmentation genes. In: *Seventh International Conference on Intelligent Systems for Molecular Biology*, pp. 195-201, Menlo Park, California: AAAI Press.

[MSKSR01] E. Myasnikova, A. Samsonova, K. Kozlov, M. Samsonova, J. Reinitz, 2001. Registration of the expression patterns of *Drosophila* segmentation genes by two independent methods. *Bioinformatics* 17(1), 3-12.

[NV96] C. Nusslein-Volhard: Gradients that organize embryo development. Scientific American. (1996) pp. 54–61

[Rec73] I. Rechenberg. *Evolutionsstrategie: Optimierung Technischer Systeme nach Prinzipien der Biologischen Evolution*. Werkstatt Bionik und Evolutionstechnik. Stuttgart: Frommann-Holzboog. 1973.

[RPJ96] R. Rivera-Pomar and H. Jäckle: ¿From gradients to stripes in *Drosophila* embryogenesis: Filling in the gaps. Trends Genet.. Vol. **12**. (1996) pp. 478–483

[Sch81] H.-P. Schwefel: *Numerical Optimization of Computer Models*, J. Wiley & Sons, New-York, 1981–1995.

[MSM97] M. Sebag, M. Schoenauer, and H. Maitournam: Parametric and non-parametric identification of macro-mechanical models. In D. Quadraglia et al., Eds, *Genetic Algorithms and Evolution Strategies in Engineering and Computer Sciences*, pp. John Wiley (1997) pp. 327–340.

[ZT98] E. Zitzler and L. Thiele: Multiobjective optimization using evolutionary algorithms - a comparative case study. In A. E. Eiben, T. Bäck , M. Schoenauer, H. P. Schwefel (Eds.) *Fifth International Conference on Parallel Problem Solving from Nature (PPSN-V)*. Springer-Verlag. (1998) pp. 292–301